

The $\alpha \rightarrow \gamma$ Transition in Ce: A Theoretical View from Optical Spectroscopy

Kristjan Haule,^{1,4} Viktor Oudovenko,^{2,4} Sergej Y. Savrasov,³ and Gabriel Kotliar⁴

¹*Jožef Stefan Institute, SI-1000 Ljubljana, Slovenia*

²*Laboratory for Theoretical Physics, Joint Institute for Nuclear Research, 141980 Dubna, Russia*

³*Department of Physics, New Jersey Institute of Technology, Newark, NJ 07102, USA*

⁴*Department of Physics and Center for Material Theory, Rutgers University, Piscataway, NJ 08854, USA*

(Received 2 March 2004; published 24 January 2005)

Using a novel approach to calculate optical properties of strongly correlated systems, we address the old question of the physical origin of the $\alpha \rightarrow \gamma$ transition in Ce. We find that the Kondo collapse model, involving both the f and the spd electrons, describes the optical data better than a Mott transition picture involving the f electrons only. Our results compare well with existing experiments on thin films. We predict the full temperature dependence of the optical spectra and find the development of a hybridization pseudogap in the vicinity of the $\alpha \rightarrow \gamma$ phase transition.

DOI: 10.1103/PhysRevLett.94.036401

PACS numbers: 71.27.+a, 71.30.+h

At a temperature of 600 K and pressure less than 20 kbar, elemental cerium undergoes a transition between two isostructural phases: a high pressure phase or α phase and a low pressure γ phase. In α -Ce the f electron is delocalized (for example, the spin susceptibility is temperature independent) while in γ -Ce the f electron is localized (for example, the electron has a Curie-like susceptibility) [1]. Several basic questions about this transition are still being debated. What is the driving mechanism of this transition? How is the electronic structure coupled to the volume changes? What is the role of the “heavy” f and the “light” spd electrons which are near the Fermi level in this material? These fundamental questions continue to be the subject of experimental investigations [2,3].

Two main theoretical hypotheses have been advanced to describe the electronic structure changes across the α - γ boundary. Johansson proposed a Mott transition scenario [4], where the transition is connected to delocalization of the f electron. In the α phase the f electron is itinerant, i.e., bandlike, while in the γ phase it is localized and hence does not participate in the bonding, explaining the volume collapse. In this picture the spd electrons are mere spectators well described by the density functional theory calculations (DFT) in the local density approximation (LDA) or its extensions.

A different view on this problem was proposed by Allen and Martin [5] and independently by Lavagna, Lacroix, and Cyrot [6], who introduced the Kondo volume collapse model. They suggested that the transition was connected with modifications in the effective hybridization of the spd bands with the f electron. The main change when going from α to γ is the degree of hybridization and hence the Kondo scale. This idea can be implemented mathematically [5,6] by estimating free energy differences between these phases by using the solution of an Anderson impurity model supplemented with elastic energy terms.

More recently, the modern dynamical mean field theory (DMFT) in combination with realistic band structure cal-

culations (LDA + DMFT) [7] was brought to bear on this problem [8,9]. LDA + DMFT allowed the computation of the photoemission spectra of cerium in both phases and the thermodynamics of the transition starting from first principles. The theoretical results were in good agreement with existing experiments [10]. The photoemission spectra close to the Fermi level are dominated by the f electron density of states. The spectrum of the α phase consists of Hubbard bands and a quasiparticle peak while the insulating γ phase has no quasiparticle or Kondo peak in the spectra and consists of Hubbard bands only. These features are consistent with both the volume collapse picture and the Mott transition picture.

In this Letter we revisit this problem theoretically using optical spectroscopy. Our qualitative idea is that the spd electrons have very large velocities, and therefore they will dominate the optical spectrum of this material. In the Mott transition picture, the spd electrons are pure spectators, and hence no appreciable changes in the optical spectrum should be observed. On the other hand, if the hybridization between the spd electrons and the f electrons increases upon entering the α phase, we expect a hybridization (pseudo)gap to develop as the temperature is lowered because spd carriers are strongly modified as they bind to the f electrons.

Formalism.—Within the LDA + DMFT method [7], the LDA Hamiltonian is superposed by a Hubbard-like local Coulomb interaction, which is the most important source of strong correlations in correlated materials and is not adequately treated within LDA alone. The resulting many-body problem is then treated in DMFT spirit, i.e., neglecting the nonlocal part of self-energy. It is well understood by now that this theory is not only exact in the limit of infinite dimensions but is also a very valuable approximation for many three-dimensional systems since it is capable of treating delocalized electrons from LDA bands as well as localized electrons on equal footing.

To calculate the central object of DMFT, the local Green's function G_{loc} , we solved the Dyson equation

$$[H_{\mathbf{k}}^{\text{LDA}} + \Sigma(\omega) - E_{\text{dc}} - \epsilon_{\mathbf{k}j\omega} O_{\mathbf{k}}] \psi_{\mathbf{k}\omega}^{R,j} = 0, \quad (1)$$

where $H_{\mathbf{k}}^{\text{LDA}}$ is the LDA Hamiltonian expressed in a localized linear muffin-tin orbital (LMTO) basis set (which we evaluated at the LDA density of cerium), $O_{\mathbf{k}}$ is the overlap matrix appearing due to nonorthogonality of the base, and $\Sigma(\omega)$ is the self-energy matrix to be determined by the DMFT. A double counting term E_{dc} appears here since the Coulomb interaction is also treated by LDA in a static way; therefore, the LDA local correlation energy has to be subtracted. Given the eigenvalues $\epsilon_{\mathbf{k}j\omega}$, the left eigenvectors $\psi_{\mathbf{k}\omega}^{L,j}$, and the right eigenvectors $\psi_{\mathbf{k}\omega}^{R,j}$ of Eq. (1) the local Green's function can be expressed by

$$G_{\text{loc},\alpha\beta} = \sum_{\mathbf{k}j} \frac{\psi_{\mathbf{k}\omega,\alpha}^{R,j} \psi_{\mathbf{k}\omega,\beta}^{L,j}}{\omega + \mu - \epsilon_{\mathbf{k}j\omega}}. \quad (2)$$

The local self-energy $\Sigma(\omega)$ that appears in Eq. (1) can be calculated from the corresponding impurity problem, defined by the DMFT self-consistency condition

$$G_{\text{loc}} = [\omega - E_{\text{imp}} - \Sigma(\omega) - \Delta_{\text{imp}}(\omega)]. \quad (3)$$

Here Δ_{imp} is the impurity hybridization matrix and E_{imp} are the impurity levels. The solution of the Anderson impurity problem, i.e., the functional $\Sigma[\Delta_{\text{imp}}(\omega), E_{\text{imp}}, U]$, closes the set of Eqs. (1)–(3).

Various many-body techniques can be used to solve the impurity problem—among others, the quantum Monte Carlo method (QMC), noncrossing approximation (NCA), or iterative perturbation theory (IPT). Here, we used one-crossing approximation (OCA) [11], which is, like NCA, based on the perturbation theory in the hybridization strength between the bath and the impurity. The lowest order self-consistent conserving approximation in this approach is the sum of all bubbles (known as NCA). The next order term in the expansion contains conduction lines that cross once. All the diagrams with singly crossed lines (that do not contain a line with more than one crossing) are summed up in the approximation [called (OCA)] [11]. The number of the crossing diagrams is very large due to the large number of pseudoparticles (2^{14}) representing the f electrons; therefore, the diagrams were generated on the computer. The OCA approximation is far superior to NCA; it considerably improves the Fermi-liquid scale T_K and reduces some pathologies of NCA, but is more time consuming. The OCA is also the lowest order self-consistent approximation exact up to $V^2 \propto \Delta_{\text{imp}}$ where Δ_{imp} is the impurity hybridization with the electronic bath.

The optical conductivity is given by the expression [12]

$$\begin{aligned} \sigma_{\mu\nu}(\omega) &= \frac{e^2}{4\pi} \sum_{ss'} \sum_{\mathbf{k}j} \int d\varepsilon \frac{f(\varepsilon^+) - f(\varepsilon^-)}{\omega} \\ &\times \frac{M_{\mathbf{k}jj'}^{ss',\mu\nu}(\varepsilon^-, \varepsilon^+)}{\omega + \epsilon_{\mathbf{k}j\varepsilon^-}^s - \epsilon_{\mathbf{k}j'\varepsilon^+}^{s'}} \\ &\times \left[\frac{1}{\varepsilon^- + \mu - \epsilon_{\mathbf{k}j\varepsilon^-}^s} - \frac{1}{\varepsilon^+ + \mu - \epsilon_{\mathbf{k}j'\varepsilon^+}^{s'}} \right], \quad (4) \end{aligned}$$

where we have denoted $\varepsilon^\pm = \varepsilon \pm \omega/2$ and used the shortcut notations $\epsilon_{\mathbf{k}j\varepsilon}^+ \equiv \epsilon_{\mathbf{k}j\varepsilon}$, $\epsilon_{\mathbf{k}j\varepsilon}^- \equiv \epsilon_{\mathbf{k}j\varepsilon}^*$. In the spirit of DMFT, the vertex corrections to the conductivity are neglected in Eq. (4). The matrix elements $M_{\mathbf{k}jj'}$ appear as standard dipole allowed transition probabilities which are now defined with the right and left solutions ψ^R and ψ^L of the Dyson equation:

$$\begin{aligned} M_{\mathbf{k}jj'}^{ss',\mu\nu}(\varepsilon^-, \varepsilon^+) &= \sum_{\alpha_1, \alpha_2} (\psi_{\mathbf{k}\varepsilon^-, \alpha_1}^{j,s})^s \nu_{\mathbf{k}\alpha_1\alpha_2}^\mu (\psi_{\mathbf{k}\varepsilon^+, \alpha_2}^{j',-s'})^{s'} \\ &\times \sum_{\alpha_3, \alpha_4} (\psi_{\mathbf{k}\varepsilon^+, \alpha_3}^{j',s'})^{s'} \nu_{\mathbf{k}\alpha_3\alpha_4}^\nu (\psi_{\mathbf{k}\varepsilon^-, \alpha_4}^{j,-s})^s, \quad (5) \end{aligned}$$

where we have denoted $\psi_{\mathbf{k}\varepsilon}^{j,+} \equiv \psi_{\mathbf{k}\varepsilon}^{j,L}$, $\psi_{\mathbf{k}\varepsilon}^{j,-} \equiv \psi_{\mathbf{k}\varepsilon}^{j,R}$, and assumed that $(\psi_{\mathbf{k}\varepsilon}^{j,s})^+ \equiv \psi_{\mathbf{k}\varepsilon}^{j,s}$ while $(\psi_{\mathbf{k}\varepsilon}^{j,s})^- \equiv (\psi_{\mathbf{k}\varepsilon}^{j,s})^*$. The expressions (4) and (5) represent generalizations of the formulas for optical conductivity for a strongly correlated system and involve the extra internal frequency integral appearing in Eq. (4).

As in previous work [8,9] we treat only the f electrons as strongly correlated thus requiring full energy resolution, while all other electrons such as Ce s , p , d are assumed to be well described by the LDA. To obtain the one particle Hamiltonian $H_{\mathbf{k}}^{\text{LDA}}$, we employed the linear muffin-tin orbital method within the atomic-spheres approximation as implemented in Ref. [13]. We used $6s$, $5p$, $5d$, and $4f$ basis functions, 4096 k points in the irreducible Brillouin zone, exchange correlation potential by Vosko *et al.*, and experimental lattice constants. Our LDA results are in good agreement with previous LDA calculations [14]. The spin-orbit coupling is taken into account; therefore, the size of the matrices in Eq. (1) is 32×32 , while the self-energy matrix appears in a sub-block of size 14×14 . The value of the Coulomb interaction U was obtained by the local density constrained occupation calculations and is shown in Fig. 5 of Ref. [15] as a function of volume. The absolute value of U in the volume range considered here is around 6 eV. The effects of the Hund's exchange J was not included in the calculation. After the self-consistency of the dynamical mean field equations is reached, the quasi-particle spectra described by $\psi_{\mathbf{k}\omega}^j$ and $\epsilon_{\mathbf{k}j\omega}$ are found, and the expression (4) for $\sigma_{\mu\nu}(\omega)$ can be evaluated. Here, we paid a special attention to the energy denominator $1/(\omega + \epsilon_{\mathbf{k}j\varepsilon^-}^s - \epsilon_{\mathbf{k}j'\varepsilon^+}^{s'})$ appearing in (4). Because of its strong \mathbf{k}

dependence the tetrahedron method of Lambin and Vigneron [16] is used. The integral over internal energy ε is calculated in an analogous way. The frequency axis is divided into a discrete set of points ε_i and assumed that the eigenvalues $\epsilon_{\mathbf{k}j\varepsilon}$ and the matrix elements $M_{\mathbf{k}jj'}^{ss',\mu\nu}(\varepsilon^-, \varepsilon^+)$ can be linearly interpolated between each pair of points. We first perform the frequency integration to convert the double pole expression (4) into a single pole expression for which the tetrahedron method is best suited.

Results and comparison with experiments.—In the top panel of Fig. 1, we present the optical conductivity obtained by the LDA + DMFT for bulk cerium while in the bottom panel the results of recent experiment on thin films [2] are reproduced. The optical conductivity of γ Ce is fairly featureless, consisting of a very broad Drude-like peak of half-width 0.4 eV on a constant background. The α phase has a much narrower Drude peak with a width of the order of 0.1 eV and a peak at 1 eV. The latter feature is remarkable because, as pointed out in Ref. [2], it indicates that when going from γ to α the electronic structure of cerium is modified on an energy scale larger than the Kondo energy. All these important qualitative features are present in both the theory and the experiment and will be interpreted theoretically below as due to excitations across a hybridization induced (pseudo)gap. Notice that, in contrast to the LDA + DMFT results, LDA predicts a narrow Drude peak in both phases [14].

In both the experiment and theory, the overall magnitude of conductivity in γ phase is smaller than in α due to the larger volume and hence reduced velocity of γ phase. There are also quantitative discrepancies between theory

and experiments. The overall magnitude of measured conductivity in both phases is approximately half of the calculated value. This discrepancy might be a consequence of neglecting Hubbard interactions among the spd electrons, an effect which would reduce the current matrix elements. Early measurements by Rhee *et al.* [17], however, suggest that the optical conductivity is a factor of 2 larger than the results of Ref. [2]. Also, both theory and experiment have a dip around 0.18 eV in the α phase, but it is much more pronounced in the LDA + DMFT calculation than in experiments.

The optical conductivity is dominated by the d bands while the photoemission spectra is dominated by the large f contribution. This is a consequence of a small overlap between neighboring f shells or, equivalently, f velocities are orders of magnitude smaller than the d velocities. However, this does not imply that the f electrons are irrelevant to the optical properties. At very high temperatures, the f electrons scatter the spd electrons, but when the temperature is lowered, they strongly hybridize or mix with the spd electrons. This results in a Kondo resonance in the f photoemission spectra and also in a hybridization (pseudo)gap in spd spectra. The traditional way to describe the low temperature state is by means of a renormalized band theory where the conductivity is given by a band theory such as the LDA with a rescaled hybridization and a shifted f level [18]. DMFT is able to describe the high temperature and the low temperature state, and in addition, add the very large lifetime effects that occur at finite temperatures and finite frequencies which are omitted in simpler treatments. To understand the optical con-

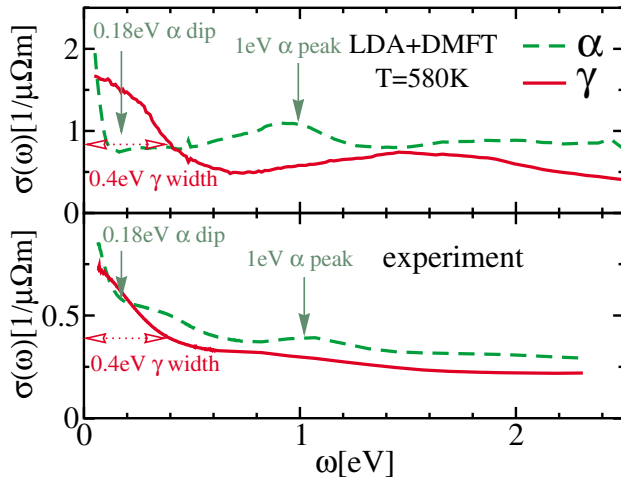


FIG. 1 (color online). The top panel shows the calculated optical conductivity for both α and γ phase of cerium. The temperature used in calculation is 580 K while the volume of α and γ phase is 28.06 \AA^3 and 34.37 \AA^3 , respectively. The bottom panel shows experimental results measured by the group of van der Marel [2]. The measurements for α phase were done at 5 K and for γ phase at 400 K.

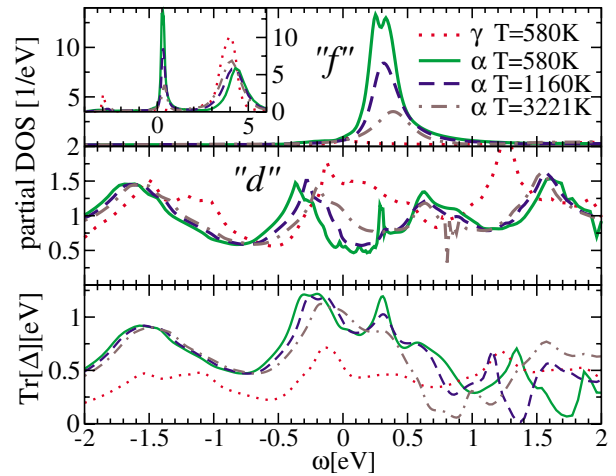


FIG. 2 (color online). Temperature dependence of partial density of states and hybridization function for both phases α and γ of Ce. The upper panel shows $L = 3$ and the middle panel $L = 2$ density of states. The lower panel shows the effective hybridization function $\text{Tr}\Delta_{\text{imp}}$. The inset shows the f density of states in the extended frequency range where also the upper Hubbard band is clearly visible.

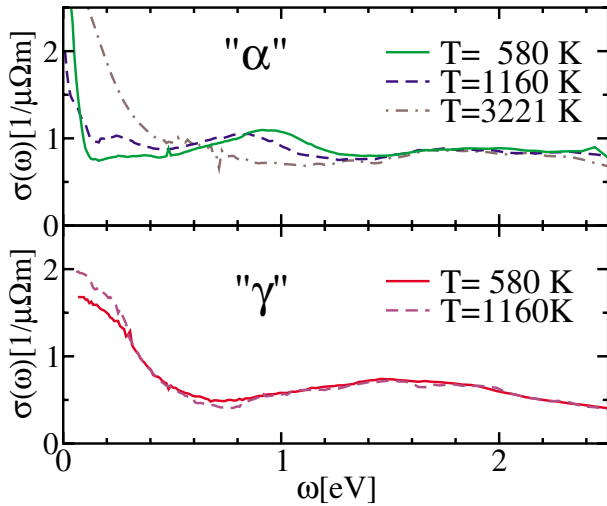


FIG. 3 (color online). Temperature dependence of optical conductivity for both phases α and γ of Ce.

ductivity, we plot the orbitally resolved density of states (DOS) in Fig. 2.

As one can see in Fig. 2, the d bands in α phase have a very pronounced hybridization (pseudo)gap which is growing by lowering temperature exactly as the Kondo peak builds up. The spectral weight is transferred from the Fermi level into the side peaks which are 1 eV apart causing 1 eV peak in optical conductivity. In the γ phase, the Kondo peak disappears because the effective hybridization of the f with spd electrons is smaller (see bottom panel of Fig. 2) and the coherence scale T_K is reduced for at least an order of magnitude. Thus, the d bands are almost decoupled from the f 's leading to a broad Drude-like peak of width 0.4 eV. In contrast, the effective hybridization obtained by the pure LDA calculation (i.e., setting $\Sigma = 0$) does not change much during the transition and remains close to the hybridization of the alpha phase.

The temperature dependence of the optical response for both the α and γ phase is shown in Fig. 3. With increasing temperature, the 1 eV peak moves to smaller frequencies and finally at few 1000 K disappears. At the same time, the hybridization (pseudo)gap below the peak gradually disappears as the temperature is raised and evolves into a broad hump, similar to the one in γ phase. This temperature dependence is easily understood by looking at the partial density of states in Fig. 2. Since the Kondo peak is gradually reduced with increasing temperature, the hybridization (pseudo)gap in d bands disappears causing featureless optical response.

The main features of the optical spectra in cerium are a consequence of a different hybridization strength in the two phases. Theory allows us to follow the development of the hybridization features as a function of temperature. The hybridization (pseudo)gap in α phase is developed at very high temperatures and hence cannot be observed experimentally in cerium. However, this could be observed in

cerium alloyed with lanthanum and thorium [19] where the Kondo scale of the α phase can be reduced enough to make the onset of hybridization experimentally observable. The hybridization (pseudo)gap was recently also observed in skutterudites [20] and previously in heavy fermion material UPt_3 [21].

Conclusion.—The methodology introduced allowed us to interpret the optical spectra of α and γ cerium, in favor of the Kondo volume collapse model. The approach outlined here will be useful for elucidating the role of the spd electrons in other materials where the f electrons are neither fully localized nor fully itinerant such as elemental plutonium and other heavy fermion compounds.

K.H. was supported by the Ministry of Education Science and Sport of Slovenia, NSF-DMR 0096462, and the Center for Materials Theory. This work was also supported by NSF-DMR Grants No. 02382188, No. 0312478, No. 0342290, DOE Grant No. DEFG02-99ER45761, the Computational Material Science Network, and DOE Grant No. LDRD-DR 200030084.

-
- [1] D. G. Koskimaki and K. A. Gschneidner, Jr., in *Handbook on the Physics and Chemistry of Rare Earths*, edited by K. A. Gschneidner, Jr. and L. R. Eyring (North-Holland, Amsterdam, 1978), p. 337.
 - [2] J. W. van der Eb, A. B. Kuz'menko, and D. van der Marel, *Phys. Rev. Lett.* **86**, 3407 (2001).
 - [3] I. K. Jeong *et al.*, *Phys. Rev. Lett.* **92**, 105702 (2004).
 - [4] B. Johansson, *Philos. Mag.* **30**, 469 (1974).
 - [5] J. W. Allen and R. M. Martin, *Phys. Rev. Lett.* **49**, 1106 (1982); J. W. Allen *et al.*, *Phys. Rev. B* **46**, 5047 (1992).
 - [6] M. Lavagna *et al.*, *Phys. Lett. A* **90**, 210 (1982).
 - [7] For recent reviews, see K. Held *et al.*, *Psi-k Newsletter* No. 56 (2003) 65; A. I. Lichtenstein, M. I. Katsnelson, and G. Kotliar, in *Electron Correlations and Materials Properties 2*, edited by A. Gonis (Kluwer, New York, 2002).
 - [8] M. B. Zöfl *et al.*, *Phys. Rev. Lett.* **87**, 276403 (2001).
 - [9] K. Held *et al.*, *Phys. Rev. Lett.* **87**, 276404 (2001); A. K. McMahan *et al.*, *Phys. Rev. B* **67**, 075108 (2003).
 - [10] D. M. Wieliczka *et al.*, *Phys. Rev. Lett.* **52**, 2180 (1984); E. Weschke *et al.*, *Phys. Rev. B* **44**, 8304 (1991); F. Patthey *et al.*, *Phys. Rev. Lett.* **55**, 1518 (1985).
 - [11] Th. Pruschke *et al.*, *Z. Phys. B* **74**, 439 (1989); K. Haule *et al.*, *Phys. Rev. B* **64**, 155111 (2001).
 - [12] V. Oudovenko *et al.*, *Phys. Rev. B* **70**, 125112 (2004).
 - [13] S. Y. Savrasov, *Phys. Rev. B* **54**, 16470 (1996).
 - [14] W. E. Pickett *et al.*, *Phys. Rev. B* **23**, 1266 (1981).
 - [15] A. K. McMahan, C. Huscroft, R. T. Scalettar, and E. L. Pollock, *J. Comput.-Aided Mater. Des.* **5**, 131 (1998).
 - [16] Ph. Lambin *et al.*, *Phys. Rev. B* **29**, 3430 (1984).
 - [17] J. Y. Rhee *et al.*, *Phys. Rev. B* **51**, 17390 (1995).
 - [18] A. J. Millis and P. A. Lee, *Phys. Rev. B* **35**, 3394 (1987); P. Coleman, *Phys. Rev. Lett.* **59**, 1026 (1987).
 - [19] B. H. Grier *et al.*, *Phys. Rev. B* **24**, 6242 (1981).
 - [20] S. V. Dordevic *et al.*, *Phys. Rev. Lett.* **86**, 684 (2001).
 - [21] S. Donovan *et al.*, *Phys. Rev. Lett.* **79**, 1401 (1997).